Available online at www.sciencedirect.com

SciVerse ScienceDirect

Energy Procedia 37 (2013) 4106 – 4113

Energy Procedia

GHGT-11

# Experimental laboratory study on the acoustic response of sandstones during injection of supercritical CO2 on CRC2 sample from Otway basin Australia

Maxim Lebedev[a]*, Vassili Mikhaltsevich[a], Olga Bilenko[b], Tess Dance[c], Marina Pervukhina[d], Boris Gurevich[a,d]

[a]*Co-operative Centre for Research Centre for Greenhouse Gas Technologies/ Department of Exploration Geophysics, Curtin University, GPO Box U1987, Perth,WA Australia*

[b]*Curtin University, GPO Box U1987, Perth, WA Australia*

[c]*Co-operative Centre for Research Centre for Greenhouse Gas Technologies /CSIRO Earth Science and Resource Engineering, 26 Dick Perry Avenue Kensington, Perth, WA Australia*

[d]*CSIRO Earth Science and Resource Engineering, 26 Dick Perry Avenue Kensington, Perth, WA Australia*

**Abstract**

Quantitative knowledge of the acoustic response of rock from an injection site on supercritical CO2 saturation is crucial for understanding the feasibility of time-lapse seismic monitoring of CO2 plume migration. A suite of shaley sandstones from the CRC-2 well, Otway Basin, Australia is tested to reveal the effects of supercritical CO2 injection on acoustic responses. The sandstone samples were cut in different directions with respect to a formation bedding plane and varied in porosities between 14% and 29% and permeabilities between 0.2 mD and 10,000 mD. Pore pressures and temperatures were varied from 4 MPa to 10 MPa, and 23°C to 45°C respectively to cover both vapour and supercritical regions of CO2 phase diagram. $CO_2$ is first injected into dry samples, flushed out with brine and then injected again into brine saturated samples. Such experimental protocol allows us to obtain acoustic velocities of the samples for the wide range of CO2 saturations from 0 to 100%. On injection of supercritical $CO_2$ ($scCO_2$) into brine-saturated samples, they exhibit observable perturbation of ~7% of compressional velocities with the increase of $CO_2$ saturation form 0% to maximum (~50%). Changes of the dry samples before and after the $CO_2$ injection (if any) are not traceable by acoustic methods. An applicability of implementation of fluid substitution using Gassmann's theory for CRC2 well has been proved in the experiments. $CO_2$ Residual saturation of about 50% was measured by monitoring of the volume of brine displaced from the sample and was independently confirmed by computer tomography (CT) imaging of the sample before and after experiments.

© 2013 The Authors. Published by Elsevier Ltd.
Selection and/or peer-review under responsibility of GHGT

Keywords: CO2; Sequestration, Rock Physics, Ultrasonic, CT

* Corresponding author. Tel.: +61 8 9266 2330; fax: +61 8 9266 3407.
*E-mail address:* m.lebedev@curtin.edu.au.

1876-6102 © 2013 The Authors. Published by Elsevier Ltd.
Selection and/or peer-review under responsibility of GHGT
doi:10.1016/j.egypro.2013.06.312

## 1. Introduction

Geologic sequestration can be considered as one of the most favourable mitigation strategies against the negative effects of atmospheric greenhouse gases, in particular carbon dioxide [1]. An ongoing project in the Otway basin, in Victoria, South Eastern Australia, is demonstrating the feasibility of geological storage of $CO_2$ in depleted fields and deep saline formations. Stage one of the CO2CRC Otway Project commenced in 2008 and has shown that $CO_2$ can be safely transported, injected and stored in a depleted gas field using a variety of monitoring techniques to verify containment [2,3]. The second stage of the CO2CRC Otway Project comprises a field scale residual saturation and dissolution test followed by injection of a small volume (10,000-30,000 tonnes) of $CO_2$ rich gas into a saline aquifer.

Laboratory measurements on available core samples provide petrophysical and geomechanical properties of the reservoir and can be used for the calibration of seismic data. Quantitative understanding of the acoustic response of sandstones from the injection site on complete or partial saturation with supercritical $CO_2$ ($scCO_2$) is important for time-lapse seismic imaging of $CO_2$ plume migration. As the injection of $scCO_2$ can potentially cause some alteration or damage of the constituent rocks, acoustic responses before and after the CO2 injection have to be tested on the core samples.

There is number of papers in which $CO_2$ injection into reservoir sandstones was studied. $CO_2$ injection into hexadecane-saturated sandstones and samples elastic responses was studied in [4]. $CO_2$ injection effects on the P-wave velocity and deformation of water-saturated Tako sandstone was reported in [5]. Experimental results of acoustic P-wave tomography for monitoring and quantification of supercritical $CO_2$ saturation during injection into brine-saturated Tako sandstone are described in [6]. Gaseous and $scCO_2$ were injected into water-saturated sandstone under controlled pressure and temperature conditions and the dependency of P-wave velocity and attenuation on saturation were monitored in [7]. A comprehensive study of $scCO_2$ injection into brine-saturated sandstone using computer tomography methods was performed in [8]. Long term effect of brine/$scCO_2$ on the mechanical properties of sandstones was reported in [9]. Recently, first measurements on samples from the CRC-1 well in the Otway Basin, Australia were reported [10].

In this work, we investigate effects of $scCO_2$ on the acoustic properties of five rock samples extracted from the CRC-2 well. This study is designed to answer three main questions: (a) What are the elastic properties of the host sandstone and can standard technique of Gassmann's fluid substitution be applied to calculate the elastic properties of saturated sandstone using standard laboratory measurements on the dry sample; (b) How will CO2 injection change acoustic velocities; and (c) Will it cause any damage in the host rock? CO2 is injected into either dry or brine saturated samples, which allowed us to obtain the acoustic velocities of the samples for the whole range of $CO_2$ saturations from 0 to 100%.

## 2. Sample description

Measurements were taken from a total of five sandstone core plug samples from the CRC-2 well. These core samples were extracted from the proposed injection interval (from 1442 to 1529 m) in the Paaratte formation, the Otway Basin. The formation itself comprises of a thick sequence of deltaic and shallow marine sediments which contain a succession of interbedded fine-to-coarse-grained quartz sandstones (potential reservoirs) and carbonaceous mudstones (baffles or seals). Five samples representing different facies were taken from the centre of the potential reservoir in order to investigate the effects of geological heterogeneity. The helium porosities and permeabilities of the samples were measured by an Automated Porosimeter (Coretest Co.) and Permeameter (AP-608) and are shown in Table 1 along with other petrophysical properties. The porosities vary from 14% to 25% and the permeabilities widely scatter from 0.2 mD to 10 000 mD. Sample 1442.1 consists of a homogeneous sandstone with only a few laminations parallel to the bedding plane. This porous and permeable

sandstone contains well sorted, fine to medium, rounded grains of predominately quartz, minor feldspar and mica matrix with kaolinite and chlorite clay as a weak cement. Sample 1500.83 is also fine-grained and well-sorted quartz sandstone, but with the occasional mottled structure from bioturbation (sand filled burrows) and small quartz pebbles. It exhibits some gradational bedding and fine cross-bedded lamination. Sample 1509.6 contains a distinct wavy carbonaceous lamination within a medium-, to very course-grained cross-stratified sandstone. Mica-rich clays, and coaly flakes are common within the quartz, feldspar and sandstone matrix. Sample 1513.82 is of a cemented sandstone. The original fabric is a very fine, to fine-grained clean quartz sandstone, but dolomite pervades throughout the pore space coating grains and reducing the porosity. Sample 1526.9 is from the Skull Creek Mudstone below the reservoir. It is poorly laminated to apparently structureless and contains abundant cm-scale, rounded to sub-rounded pyrite nodules and intense bioturbation.

## 3. Experiment

The rock physics tests were conducted using a triaxial (Hoek) high pressure cell with a capacity of up to 70 MPa, with capability for measurements of up to 150 MPa axial load, 70 MPa confining pressure and up to 20 MPa pore pressure. Confining ($P_{conf}$) and axial ($P_{ax}$) pressures were applied to the jacketed sample and were controlled using hydraulic hand pumps. The error in pressure determination was less than 0.25 MPa. In these tests, axial pressure was equal to confining pressure. The core flooding equipment comprises of a $CO_2$ cylinder, a $CO_2$ syringe pump, a high pressure cell, an ultrasonic system and a pump for brine injection. The temperature range is varied from room temperature up to 80°C.

To flood a sample with brine a "liquid" pump (Shimazu) was used. Carbon dioxide in vapour or supercritical phases ($scCO_2$) was injected into the sample using syringe pump (ISCO-Teledyne). The $scCO_2$ was then transported via heated pipes into the high pressure cell. To maintain pore pressure inside the sample during testing, a relief valve was installed in the outlet of the pressure cell. Syringe pump, tubes, and high pressure cell were heated and maintained at a temperature of 45 ± 0.3°C

The ultrasonic system performs precise measurements of compressional (P-) and shear (S-) waves in the axial direction using "time of flight" method. Ultrasonic waveforms, both P-wave and S-wave, were recorded at each effective pressure ($P_{eff}$). Effective pressure ($P_{eff}$) is defined as

$$P_{eff}=P_{conf}-\alpha P_{pore} \quad (1)$$

their α is a coefficient of fluid interaction with rock matrix, we assumed that α is equal to 1 (weak fluid-matrix interaction, which generally can be not a case for $scCO_2$ fluids). Nominal pulse centre frequency of transducers was 0.5 MHz for both P and S waves. Ultrasonic pulses were generated and signals were recorded using a 5077PR Pulser and Receiver unit (Panametrics) and were registered using digital oscilloscope TDS3031 (Tektronix).

Table 1. Petrophysical properties of the samples

| Core sample | Cutting direction** | Density, kg/m3 | Porosity, % | Permeability, $m^2$ |
|---|---|---|---|---|
| 1442.1 | H | 1809 | 26* | $10^{-11}$ |
| 1500.83 | V | 1806 | 24.69 | $5.5\cdot10^{-12}$ |
| 1509.6 | V | 1947 | 25.33 | $1.2\cdot10^{-13}$ |
| 1513.82 | V | 2142 | 16.14 | $1.7\cdot10^{-14}$ |
| 1526.9 | V | 2178 | 14.23 | $1.9\cdot10^{-16}$ |

* Estimation from log data

** H and V mean that the sample is cut parallel or normal to bedding, respectively.

Ultrasonic velocities are measured for dry samples (i.e. with air as a pore fluid inside sample), fully saturated with brine (salinity of brine used is 1500 ppm of 50% NaCl and 50% KCl, which is typical for the field conditions), fully saturated with $scCO_2$, and during $scCO_2$ injection into brine saturated samples. All experimental system is heated heated up to 45 °C.

Residual $scCO_2$ saturation in the sample is estimated by measuring the amount of brine volume removed (and collected) from the sample. The total amount of $CO_2$ stored in the sample (the volume of $scCO_2$ and amount of $CO_2$ dissolved in the brine) is estimated by weighing the sample after the CO2 injection and at the end of the experiment when the pore pressure reduced and the $CO_2$ released from the sample.

Computer tomography (CT) was used to observe damages of the sample by flooding, to determine porosity map and obtain a distribution of brine after experiments. Samples were scanned at ambient conditions using a medical CT scanner (Toshiba) with spatial resolution of 1mm x 1mm x 1mm, distance between scans was 1 mm. Samples were scanned before experiments (dry sample), after $CO_2$ injection into brine and in 100% brine saturated conditions. No any additives in order to increase X-ray adsorption were dissolved in the brine, in order to avoid any chemical reactions of such additive with rock matrix to keep samples undamaged. Image processing was done using open software ImageJ.

## 4. Result and discussion

The obtained results are illustrated hereafter on the 1500.83 sample but the detailed description of the results acquired on other samples is given. Figure 1 shows ultrasonic P- and S- velocities measured on the dry and brine-saturated 1500.83 sample at different confining and pore pressures. The results are presented against the effective pressure. Velocities measured on dry sandstones at stresses of 10–20 MPa exponentially saturate by a linear trend that is observable at higher stresses. Such stress dependencies are typical for sandstones and can be empirically described with relations [11], explained theoretically with the dual-porosity model developed at [12] and confirmed in a number of works afterwards [13,14]. Laboratory measurements and field data (log) are shown in the Fig. 2.

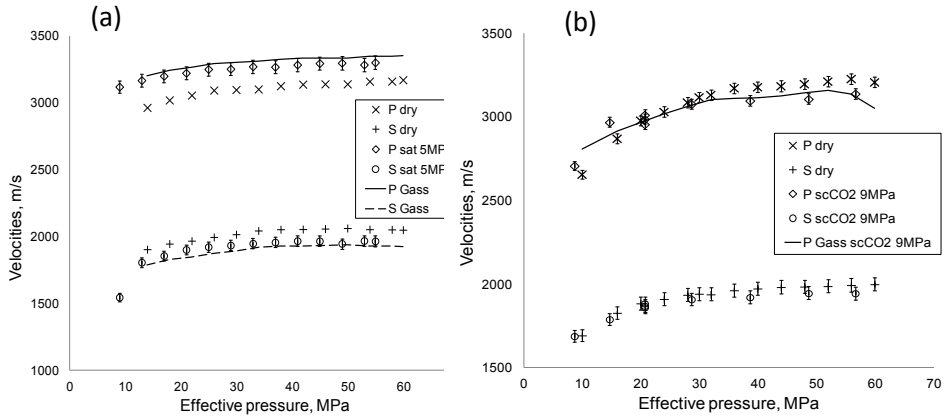


Fig. 1. (a) P-wave and S-wave velocities and Gassmann fluid substitution (brine) for CRC-2 reservoir sandstone excavated from the depth of 1500.83 m. T=45°C ; (b) P-wave and S-wave velocities and Gassmann fluid substitution (brine) for sample 1500.83 m: dry and $scCO_2$ saturated T=45°C

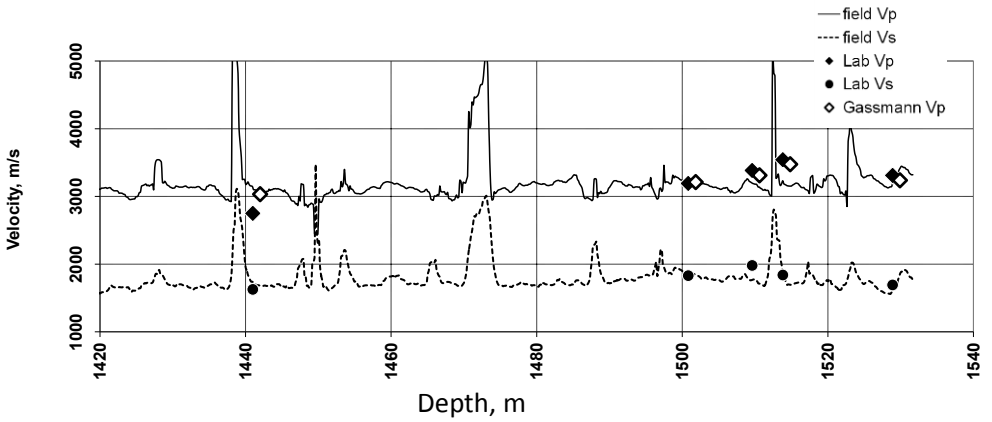


Fig. 2. P and S waves velocities measured in the field (log data), in the laboratory for brine saturated samples (at reservoir conditions), and results of Glassman fluid substitution model from laboratory measurements.

Experimentally measured velocities are in a good agreement with velocities calculated from dry velocities using Gassmann's relations for all the samples that are cut normal to bedding. It is worth noting that while for effective pressures above 20 MPa the differences between velocities measured on saturated samples and obtained with Gassmann's substitution are within the experimental errors, the velocities measured for lower stresses substantially exceed Gassmann's predictions. This fact can be explained with the local squirt theory [15] which predicts increase of rock elastic moduli at ultrasonic frequencies. At the ultrasonic frequencies used in the experiment (0.5 MHz), local pressure has no time to equilibrate between equant pores with aspect ratios of ~1 and the ultra-thin pores with aspect ratios of less than about 0.001 These ultra-thin pores are also compliant and typically get closed at low effective stresses (~20 MPa for the samples of interest) and so at the higher stresses local squirt does not affect elastic properties anymore and velocities of saturated rock can be calculated from the measurements on dry samples using Gassmann's equations.

Gassmann's predictions strongly overestimate P-wave velocities experimentally measured on the brine saturated sample 1442.1, which is cut parallel to bedding. This sample is first saturated with gaseous $CO_2$ that becomes supercritical when the pore pressure is increased and reaches 9.3 MPa. The pressure is then released and eventually the sample is flooded with brine. The deviation from Gassmann's predictions of the velocities measured on the saturated sample can be explained by the fact that the sample is rich in weak clay cement which could be overdried and destroyed with $CO_2$ injection and the subsequent pore pressure increase. At the same time, S-wave velocity changes are in a good agreement with the predicted changes due to change in density and do not exhibit any damage.

Ultrasonic velocities measured during the injection of $scCO_2$ into a brine saturated sample at confining stress of 30 MPa and pore pressure of 9.3 MPa are shown in Figure 3 for samples 1500.83 and 1442.1. For both samples, 1442.1 and 1500.83, scCO2 saturation up to ~50% is reached; the velocities at 100% of $scCO_2$ saturation are taken from the previous experiment on the injection of $scCO_2$ into a dry sample. In the case of sample 1500.83, the compressional velocity decreases almost linearly with the increase of $scCO_2$ saturation. At the maximum saturation of ~50% reachable at this experiments, $V_P$ still exceeds P-wave velocity at 100% $scCO_2$ saturated sample on about 50 m/s. The overall increase in shear velocity is caused by density decrease and does not exceed 70 m/s or ~4% of the initial S-wave velocity. For sample 1442.1 the compressional velocity remains constant up to the $scCO_2$ concentration of about 20% and then abruptly drops. With the further increase of $scCO_2$ saturation from 30% to 100%, the velocity does not

change (within the accuracy of experimental measurements). The overall drops in compressional velocities when the $scCO_2$ saturation increases from 0 to 50% is ~7% for both samples and with the further increase of the $scCO_2$ saturation, $V_P$ drops 0% and 3% for samples 1442.1 and 1500.83, respectively. The changes in ultrasonic velocities due to the $scCO_2$ saturation are noticeably different for these two samples. It is worth noting that the orientation of the samples is different, namely, sample 1442.1 is cut parallel to the bedding plane while sample 1500.83 is cut perpendicular to it.

Finally, compressional and shear velocities of the dry sample 1500.87 before and after the CO2 injection are shown in Fig. 4. The observed changes are small and within the experimental errors. This fact shows that $scCO_2$ injection in this sample has caused no damage or alteration or this alteration is not detectable by acoustic methods. Dry velocities after the $CO_2$ injection have been measured for one sample only and further measurements are necessary to verify this conclusion.

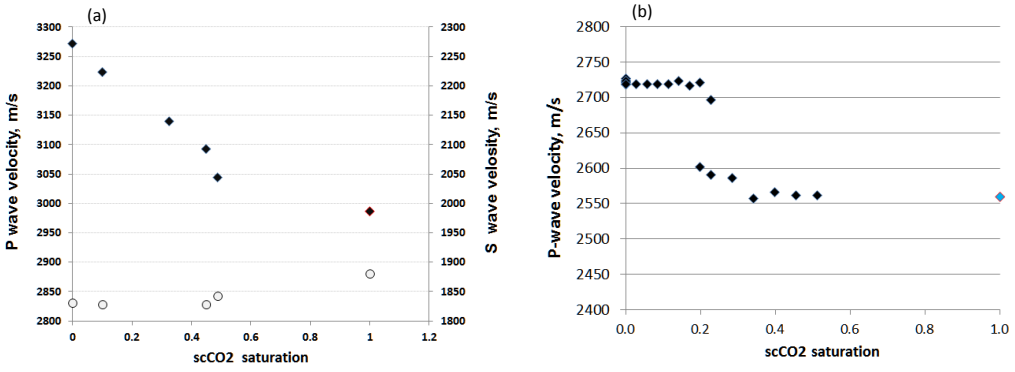


Fig. 3. Ultrasonic velocities vs. $scCO_2$ saturation for samples: a) 1500.83 and b) 1442,1. Velocities measured during scCO2 injection into brine-saturated sandstone at a temperature of 45° C, confining pressure of 30 MPa and pore pressure and $scCO_2$ injection pressure of of 9.3 MPa. Velocities corresponding to saturation 1 (100% $scCO_2$ saturation) are taken from the Fig 1 (b).

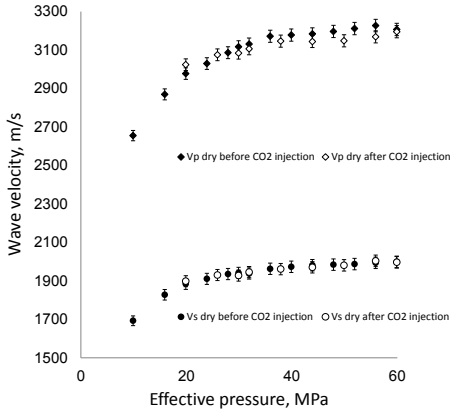


Fig. 4. Ultrasonic velocities measured on dry sample 1500.83 before and after the experiments.

Fig. 5 shows results of CT scanning of a typical sandstone sample. For each slices, a porosity distribution (porosity map) was obtained by subtracting "dry image" of the slices from its "100% brine saturated image" and is shown in the Fig 5 a). Brighter colours indicate more porous parts of the sample. Combined 3D image of porosity map was created and its side view shown in the Fig 5 c).

Residual $CO_2$ distribution, which is an inverse of a brine distribution, for each slice was obtained by subtracting images obtained after CO2 injection from the images of 100% brine saturated sample. Residual $CO_2$ distribution in the sample is presented in the Fig. 5 b). Brighter colours show the parts with more $CO_2$ saturation. Combined 3D image of $CO_2$ saturation is presented in the Fig. 5 d). It was qualitatively observed that pores in the sample are distributed not homogenously, but formed more porous and less porous areas parallel to bedding. $CO_2$ saturation (volume of $CO_2$ / total volume of pore) of more porous parts is higher than less porous. Such non-homogeneous distribution of brine and $CO_2$ inside sample can lead to dramatic increasing of attenuation of waves [16] which was observed in this work and will be studied in details in the future.

## Conclusions

Supercritical $CO_2$ injection experiments are carried out a suite of shaley sandstone specimens from the CRC2 well, Otway basin. The experiments confirm applicability of the Gassmann's fluid substitution method to brine (for four out of five samples) and to $scCO_2$ (for both tested samples). On injection of $scCO_2$ into brine-saturated samples, they exhibit observable perturbation of ~7% of compressional velocities with the increase of $CO_2$ saturation form 0% to maximum (~50%). Finally, the acoustic velocities measured on the dry samples before and after the $CO_2$ injection show no noticeable difference, which implies no damage or alteration due to the injection.

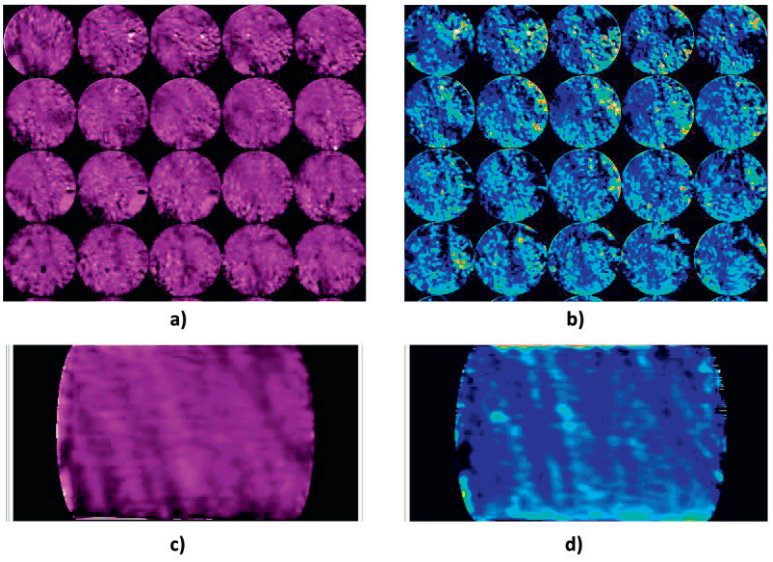


Fig. 5. a) Montage of slices of porosity: distance between slices is 1 mm, brighter colours indicated more porous part, darker parts are less porous, b) montage of slices of CO2 distribution after injection into brine saturated sample: brighter colour shows more $CO_2$; c) 3D image of porosity distribution, d) 3D image of $CO_2$ distribution. Images were processed using open software ImageJ.

## Acknowledgements

This work was partially funded by the Australian Commonwealth Government through the Cooperative Research Centre for Greenhouse Gas Technologies (CO2CRC) and by the sponsors of the Curtin Reservoir Geophysics Consortium (CRGC). Authors would like to thank Charles Jenkins (CSIRO) for ongoing discussions and valuable suggestions.

## References

[1] Schrag DP. Preparing to capture carbon: *Science* 2007;**315**:812-813.

[2] Underschultz J, Boreham JC, Dance T, Stalker L, Freifeld B, Kirste D, Ennis-King J. CO2 storage in a depleted gas field: an overview of the CO2CRC Otway Project and initial results: *Int J Greenhouse Gas Control* 2011;**5**:922-932.

[3] Jenkins CR, Cook PJ, Ennis-King J, Underschultz J, Boreham C, Dance T, De Caritat P, Etheridge DM, Freifeld BM, Hortle A, Kirste D, Paterson L, Pevzner R, Schacht U, Sharma S, Stalker L, Urosevic M. Safe storage and effective monitoring of CO2 in depleted gas fields. *Proc National Acad Sci* 2012;**109:** E35-E41.

[4] Wang Z, Nur A. Effect of CO2 flooding on wave velocities in rocks and hydrocarbons. *Soc Petr Eng Res Eng* 1989:**3**:429-439.

[5] Xue Z., Ohsumi T., Seismic wave monitoring of CO2 migration in watersaturated porous sandstone. *Explorations Geophysics* 2004;**35**: 25–32.

[6] Shi JQ, Xue Z, Durucan S. Seismic monitoring and modelling of supercritical CO2 injection into a water-saturated sandstone: Interpretation of P-wave velocity data. *Int J Greenhouse Gas Control* 2007; **1:**473-480.

[7] Lei X, Xue Z. Ultrasonic velocity and attenuation during CO2 injection into water-saturated porous sandstone: Measurements using difference seismic tomography. *Physics of the Earth and Planetary Interiors* 2009;**176**: 224–234.

[8] Shi JQ, Xue Z, Durucan S. Supercritical CO2 core flooding and imbibition in Tako sandstone–Influence of sub-core scale heterogeneity. *Int J Greenhouse Gas Control* 2011; **5**: 75-87.

[9] Zemke K, Liebscher A, Wandrey M. Petrophysical analysis to investigate the effects of carbon dioxide storage in a subsurface saline aquifer at Ketzin, Germany (CO2SINK): *Int J Greenhouse Gas Control* 2010:**4**: 990-999.

[10] Siggins AF, Lwin M, Wisman P. Laboratory calibration of the seismo-acoustic response of CO2 saturated sandstones. *Int J Greenhouse Gas Control* 2010;**4**: 920-927.

[11] Eberhart-Phillips D, Han DH, Zoback MD. Empirical relationships among seismic velocity, effective pressure, porosity and clay content in sandstone. *Geophysics* 1989;**54**: 82-89.

[12] Shapiro SA. Elastic piezosensitivity of porous and fractured rocks. *Geophysics* 2003; **68**:482-486.

[13] Becker K, Shapiro SA, Stanchits S, Dresen G, Vinciguerra S. Stress induced elastic anisotropy of the Etnean basalt: Theoretical and laboratory examination. *Geophys Res Lett* 2007;**34**:L11307.

[14] Pervukhina M, Gurevich B, Dewhurst D N, Siggins AF. Applicability of velocity–stress relationships based on the dual porosity concept to isotropic porous rocks. *Geophysical Journal International* 2010;**181**:1473–1479.

[15] Mavko G, Jizba D. Estimating grain-scale fluid effects on velocity dispersion in rocks. *Geophysics* 1991;**56**:1940-1949.

[16] Müller TM, Gurevich B, Lebedev M. Seismic wave attenuation and dispersion resulting from wave-induced flow in porous rocks — A review. *Geophysics* 2010;**75**:75147-75164